Such subtle changes, for instance, can originate from different interactions of the membrane-mimicking environment (amphipols or nanodiscs) with helices S1–S3. These helices contain the largest number of membrane lipid-facing residues (69%), of which only 80% are identical between rTRPV6 and hTRPV6.

To understand the structural changes that occur during TRPV6 opening, we compared our hTRPV6(R470E) and hTRPV6 structures. The principal changes occur in the pore-lining helix S6 and originate at A566, which is highly conserved in TRPV5 and TRPV6 (Extended Data Fig. 9k) and located right below the selectivity filter (Fig. 3g). Confirming its important role in gating, substitution of A566 with threonine, the homologous residue conserved in TRPV1–4, greatly reduced the TRPV6 current amplitude (Extended Data Fig. 1d) and slowed calcium uptake by approximately 30 times (Extended Data Fig. 1e, h). Upon opening, S6, which has an α-helical conformation in the closed state, undergoes a local transition to a π-helix. Notably, such a transition has been hypothesized previously, based on a comparison between the TRPV1 and TRPV2 structures[21]. Concurrently, the lower part of S6, which forms the gate in the closed state, rotates by about 100° and bends away from the pore axis by about 11° (Fig. 3g). These rearrangements not only widen the pore for permeant ions but also change the set of residues that face the pore axis (for example, N572 and I575 in the open state compared to L574 and M578 in the closed state). Alanine A566, therefore, acts as a hinge to allow TRPV6 gating at the S6 bundle crossing without changing the conformation of the selectivity filter (Fig. 3f). Correspondingly, the selectivity filter appears to play a crucial role in TRPV6 channel ion permeation rather than gating. Gating-related conformational changes induced by the α-to-π-helical transition in S6 seem to involve only the intracellular portions of S5 and S6, the S4–S5 linker and the TRP helix. Indeed, superposition of the corresponding regions (residues 469–500 plus 566–608) in hTRPV6 and hTRPV6(R470E) gives an r.m.s.d. of 1.74 Å, while the rest of the molecules superpose with a much lower r.m.s.d. of 0.218 Å.

Within the regions involved in gating, pore opening in hTRPV6 is accompanied by the formation of two electrostatic bonds per subunit (Fig. 4b). A salt bridge forms between Q473 in the S4–S5 elbow and R589 in the TRP helix, and a hydrogen bond forms between D489 in the S5 helix and T581 in the S6 helix. Neither interaction is present in the closed-state structures of hTRPV6(R470E) or rTRPV6 and the formation of the hydrogen bond (D489–T581 in hTRPV6(R470E) or D488–T580 in rTRPV6) is prevented by the side chain of M577 or M576, respectively (Fig. 4c, d, Extended Data Fig. 8f, g). The importance of the D489–T581 interaction for hTRPV6 opening is supported by the previous observation that a mutation equivalent to T581A reduces the excessive constitutive activity of an hTRPV6(G516S) mutant[22]. We speculate that formation of the electrostatic bonds compensates for the energetic cost of the unfavourable α-to-π-helical transition in S6 during channel opening. This structural solution therefore maintains the relative stabilities and similar energy levels of both gating states and supports the constitutive activity of TRPV6. Accordingly, the open and closed conformations of TRPV6 remain in a readily tunable equilibrium that can be shifted towards either state by different stimuli, including lipids[7,9].

Our structures of hTRPV6 reveal a gating mechanism that is novel among tetrameric ion channels (Fig. 5, Supplementary Video 1). Although other representatives of the TRP channel family have a local α-to-π-helical transition in the middle of S6[18,23–25], they lack the alanine gating hinge (Extended Data Fig. 9). As a result, S6 maintains its secondary structure throughout the entire TRPV1 gating cycle, the same residues face the pore in the closed and open states, and pore widening is observed at both the S6 bundle crossing and the selectivity filter[18]. On the other hand, K^+ channels do have a gating hinge in their pore-forming inner helices[26,27]. However, this hinge is formed by a glycine located one residue C-terminally compared to the gating hinge alanine in TRPV6 and permits bending of the inner helices by about 30° without an α-to-π transition. The glycine hinge, like the alanine hinge in TRPV6, allows gating of K^+ channels to occur at the inner helices bundle crossing without changing the selectivity filter. However, unlike TRPV6, the glycine gating hinge in K^+ channels does not introduce a 100° rotation of the lower parts of the pore-forming helices and correspondingly does not change the residues that line the pore gate region. An alanine gating hinge is present in the pore-forming helices of ionotropic glutamate receptor (iGluR) family tetrameric ion channels[28]. However, this alanine gating hinge is located at the ion channel gate region. Correspondingly, bending the pore-forming helices at the iGluR alanine gating hinge directly alters the diameter of the pore in close proximity to the gate without an α-to-π transition. The alanine gating hinge in TRPV5 and TRPV6 channels is therefore a unique structural element that is likely to be associated with their exclusive physiological role as constitutively active calcium uptake channels.

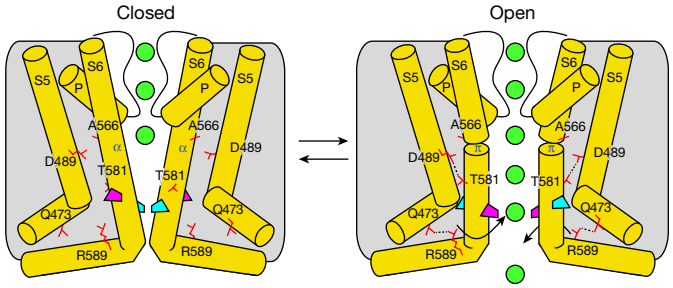

Figure 5 | TRPV6 channel gating mechanism. Cartoons represent the structural changes associated with TRPV6 channel gating. Transition from the closed to open state, stabilized by the formation of salt bridges (dashed lines), leads to permeation of ions (green spheres) and is accompanied by a local α-to-π-helical transition in S6 that maintains the selectivity filter conformation, while the lower part of S6 bends by about 11° and rotates by about 100°. These movements result in a different set of residues (cyan versus pink symbols) lining the pore in the vicinity of the channel gate.

Online Content Methods, along with any additional Extended Data display items and Source Data, are available in the online version of the paper; references unique to these sections appear only in the online paper.

Received 14 August; accepted 28 November 2017.
Published online 20 December 2017.

1. Peng, J. B. *et al.* Molecular cloning and characterization of a channel-like transporter mediating intestinal calcium absorption. *J. Biol. Chem.* **274,** 22739–22746 (1999).
2. Yue, L., Peng, J. B., Hediger, M. A. & Clapham, D. E. CaT1 manifests the pore properties of the calcium-release-activated calcium channel. *Nature* **410,** 705–709 (2001).
3. Owsianik, G., Talavera, K., Voets, T. & Nilius, B. Permeation and selectivity of TRP channels. *Annu. Rev. Physiol.* **68,** 685–717 (2006).
4. Woudenberg-Vrenken, T. E. *et al.* Functional TRPV6 channels are crucial for transepithelial Ca^{2+} absorption. *Am. J. Physiol. Gastrointest. Liver Physiol.* **303,** G879–G885 (2012).
5. Fecher-Trost, C., Weissgerber, P. & Wissenbach, U. TRPV6 channels. *Handb. Exp. Pharmacol.* **222,** 359–384 (2014).
6. Lehen'kyi, V., Raphaël, M. & Prevarskaya, N. The role of the TRPV6 channel in cancer. *J. Physiol. (Lond.)* **590,** 1369–1376 (2012).
7. Zakharian, E., Cao, C. & Rohacs, T. Intracellular ATP supports TRPV6 activity via lipid kinases and the generation of $PtdIns(4,5)P_2$. *FASEB J.* **25,** 3915–3928 (2011).
8. den Dekker, E., Hoenderop, J. G., Nilius, B. & Bindels, R. J. The epithelial calcium channels, TRPV5 & TRPV6: from identification towards regulation. *Cell Calcium* **33,** 497–507 (2003).
9. Velisetty, P. *et al.* A molecular determinant of phosphoinositide affinity in mammalian TRPV channels. *Sci. Rep.* **6,** 27652 (2016).
10. Singh, A. K., Saotome, K. & Sobolevsky, A. I. Swapping of transmembrane domains in the epithelial calcium channel TRPV6. *Sci. Rep.* **7,** 10669 (2017).
11. Saotome, K., Singh, A. K., Yelshanskaya, M. V. & Sobolevsky, A. I. Crystal structure of the epithelial calcium channel TRPV6. *Nature* **534,** 506–511 (2016).
12. Bödding, M. & Flockerzi, V. Ca^{2+} dependence of the Ca^{2+}-selective TRPV6 channel. *J. Biol. Chem.* **279,** 36546–36552 (2004).
13. Hoenderop, J. G., Nilius, B. & Bindels, R. J. Calcium absorption across epithelia. *Physiol. Rev.* **85,** 373–422 (2005).